

## Supporting Information

### **Cu Doping in FeP Enabling Efficient Electrochemical Nitrate Reduction to Ammonia in Neutral Media**

*Bo Li, <sup>a</sup> Pengfei Xue, <sup>a</sup> Man Qiao, <sup>a</sup> Yujia Tang, <sup>a</sup> and Dongdong Zhu<sup>\*ab</sup>*

<sup>a</sup> School of Chemistry and Materials Science, Institute of Advanced Materials and Flexible Electronics (IAMFE), Nanjing University of Information Science and Technology, Nanjing, 210044, China. E-mail: dd.zhu@nuist.edu.cn

<sup>b</sup> Anhui Laboratory of Molecule-Based Materials, College of Chemistry and Materials Sciences, Anhui Normal University, Wuhu, 241002, China

## 1. Experimental section

### 1.1 Materials

Iron nitrate nonahydrate ( $\text{Fe}(\text{NO}_3)_3 \cdot 9\text{H}_2\text{O}$ ), urea ( $\text{CO}(\text{NH}_2)_2$ ), ammonium fluoride ( $\text{NH}_4\text{F}$ ), Copper(II) Chloride Dihydrate ( $\text{CuCl}_2 \cdot 2\text{H}_2\text{O}$ ), Sodium hypophosphite monohydrate ( $\text{NaH}_2\text{PO}_2 \cdot \text{H}_2\text{O}$ ), Sodium nitrate ( $\text{NaNO}_3$ ), sodium nitrite ( $\text{NaNO}_2$ ), sodium sulfate ( $\text{Na}_2\text{SO}_4$ ), ammonium chloride ( $\text{NH}_4\text{Cl}$ ), sodium hydroxide ( $\text{NaOH}$ ), sodium nitroferricyanide dihydrate ( $\text{C}_5\text{FeN}_6\text{Na}_2\text{O} \cdot 2\text{H}_2\text{O}$ ), sulfamic acid solution ( $\text{H}_3\text{NO}_3\text{S}$ ), ammonium chloride ( $\text{NH}_4\text{Cl}$ ), sodium salicylate ( $\text{C}_7\text{H}_5\text{NaO}_3$ ), trisodium citrate dihydrate ( $\text{C}_6\text{H}_5\text{Na}_3\text{O}_7 \cdot 2\text{H}_2\text{O}$ ), sodium hypochlorite solution ( $\text{NaClO}$ ), and N-(1-naphthyl) ethylenediamine dihydrochloride ( $\text{C}_{12}\text{H}_{14}\text{N}_2$ ) were purchased from Aladdin Ltd. (Shanghai, China). Sulfuric acid ( $\text{H}_2\text{SO}_4$ ), hydrochloric acid ( $\text{HCl}$ ) and ethanol ( $\text{C}_2\text{H}_5\text{OH}$ ) were bought from China National Pharmaceutical Group Corp. (China). All reagents used in this work were of analytical grade and were not further purified.

### 1.2 Preparation of Cu-FeP and FeP

In brief, Cu-FeP catalyst grown on carbon cloth was prepared as follows: Firstly, 2.5 mmol of  $\text{Fe}(\text{NO}_3)_3 \cdot 9\text{H}_2\text{O}$ , 5.0 mmol of  $\text{NH}_4\text{F}$  and 12.5 mmol of urea were dissolved in 35.0 mL deionized water under stirring for 20 min. A piece of pretreated CC ( $3 \times 3 \text{ cm}^2$ ) substrate was immersed into the solution and transferred into a 50.0 mL Teflon-lined autoclave. The Teflon-

lined autoclave was then sealed and maintained at 120 °C for 6 h. After the autoclave cooled down naturally to room temperature, the Fe-based precursor on CC was taken out, washed with distilled water and anhydrous ethanol for several times. Secondly, the as-obtained Fe-based precursor was soaked in 10.0 mM CuCl<sub>2</sub> solution for 12 h to undergo a cation exchange process. After cation exchange, the sample was taken out from the solution and washed with distilled water for several times, followed by drying at 60 °C for 1.5 h. Finally, the dried sample was treated by low-temperature phosphorization at 350 °C for 5 h in Ar gas stream, and 0.5 g NaH<sub>2</sub>PO<sub>2</sub>·H<sub>2</sub>O was used as the phosphorus source. Since the as-generated PH<sub>3</sub> from NaH<sub>2</sub>PO<sub>2</sub>·H<sub>2</sub>O is harmful to human health, it is required to use CuSO<sub>4</sub> solution to absorb the unreacted PH<sub>3</sub> in the tail gas. FeP sample was prepared via directly phosphating Fe-based precursor at 350 °C for 5 h in Ar gas stream.

### **1.3 Electrochemical measurements**

All electrochemical measurements were performed in an H-type electrochemical cell at the CHI 760E electrochemical workstation (Chen Hua, Shanghai), using a standard three-electrode setup under the ambient conditions. The electrolyte was 0.25 M Na<sub>2</sub>SO<sub>4</sub> with 2000 ppm NO<sub>3</sub><sup>-</sup>, using Cu-FeP/CC (0.25 cm<sup>2</sup>) as the working electrode, platinum foil as the counter electrode, and saturated calomel electrode (SCE) as the reference

electrode. All potentials were recorded against the reversible hydrogen electrode (RHE), and no IR correction was applied for the presented potentials. The potentiostatic test was carried out at different potentials for 1.0 h with a stirring rate of 350 rpm.

#### **1.4 Determination of $\text{NH}_3$**

The  $\text{NH}_3$  concentration was determined by the indophenol blue method. Firstly, 5.0 g of trisodium citrate dihydrate and 5.0 g of sodium salicylate were dissolved in 100.0 mL of 1.0 M NaOH (Reagent A). Reagent B was 0.05 M NaClO. Reagent C was 0.20 g of sodium nitroferricyanide mixed with 20.0 mL of deionized water. Secondly, a certain amount of electrolyte was taken out from the electrolytic cell and diluted to detection range. Afterwards, 2.0 mL dilution solution was added with 2.0 mL Reagent A, 1.0 mL Reagent B, and 0.20 mL Reagent C. After standing in the dark for 2 h, the UV-Vis absorbance was measured at a wavelength of 655 nm. The concentration-absorbance curve was calibrated using the standard  $\text{NH}_4\text{Cl}$  solution with concentrations of 0, 0.50, 1.00, 2.00, and 3.00 ppm of 0.25 M  $\text{Na}_2\text{SO}_4$  solution.

#### **1.5 Determination of $\text{NO}_2^-$**

The  $\text{NO}_2^-$  concentration was detected according to the method of Griess. Firstly, sulfanilamide solution (reagent A) was 0.50 g of sulfanilamide

dissolved in 50.0 mL of 2.0 M HCl solution. Reagent B was 20.0 mg of N-(1-Naphthyl) ethylenediamine dihydrochloride mixed with 20.0 mL of deionized water. Secondly, a certain amount of electrolyte was taken out from the electrolytic cell and diluted to 5.0 mL to detection range. Next, 0.1 mL of reagent A were immersed into the dilution solution (5.0 mL). After standing for 10 minutes, 0.1 mL of reagent B were immersed into the dilution solution. After standing for 30 minutes at room temperature, the ultraviolet-visible absorption was measured at a wavelength of 540 nm and 650 nm. The final absorbance value is the difference between at 540 nm and 650 nm. The concentration-absorbance curve was calibrated using the standard  $\text{NaNO}_2$  solution with different concentrations.

### **1.6 Determination of FE and $\text{NH}_3$ yield**

$$\text{FE} = (8 \times F \times C \times V) / (M_{\text{NH}_3} \times Q) \times 100\%$$

$$\text{NH}_3 \text{ yield} = (C \times V) / (M_{\text{NH}_3} \times T \times A)$$

Where F is the Faradic constant ( $96485 \text{ C mol}^{-1}$ ), C is the measured  $\text{NH}_3$  concentration, V is the volume of electrolyte in the anode compartment (40 mL),  $M_{\text{NH}_3}$  is the molar mass of  $\text{NH}_3$ , Q is the total quantity of applied electricity, t is the electrolysis time (1.0 h), A is the loaded area of catalyst ( $0.5 \times 0.5 \text{ cm}^2$ ).

## 2. Supplementary Figures and Table

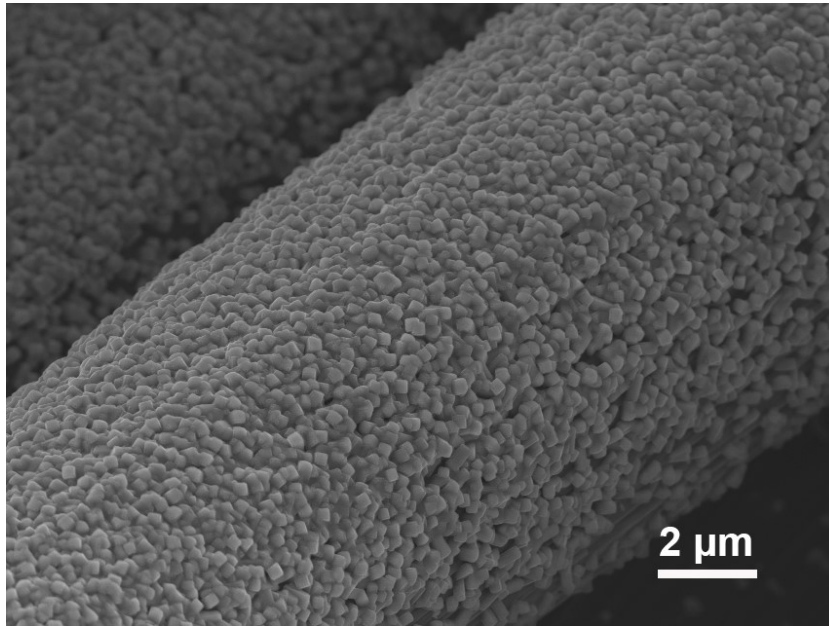


Figure S1. SEM image of FeP.

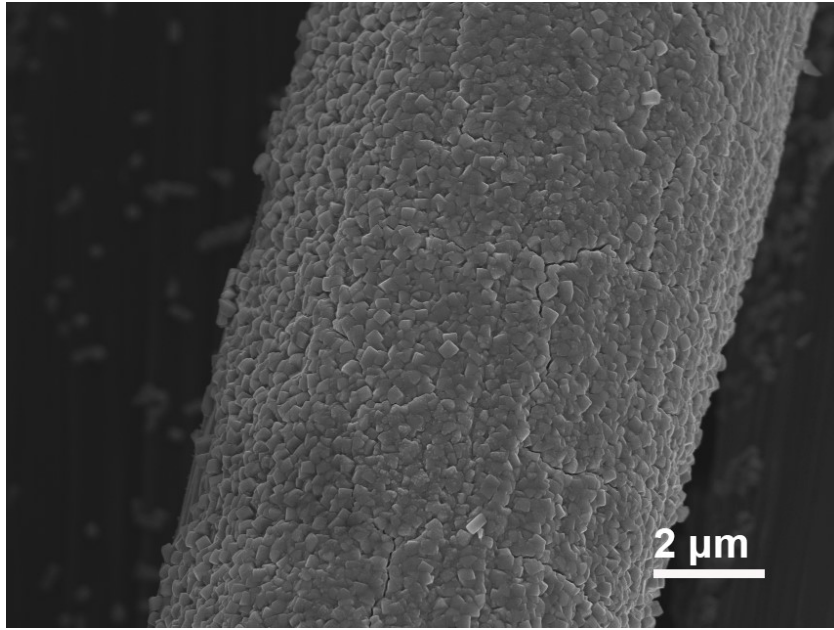


Figure S2. SEM image of Cu-FeP.

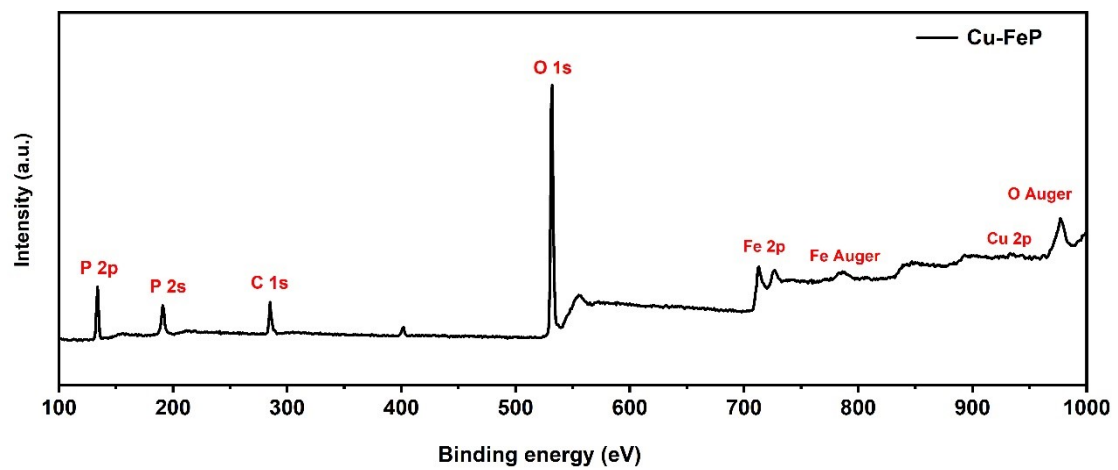


Figure S3. XPS survey spectrum of Cu-FeP.

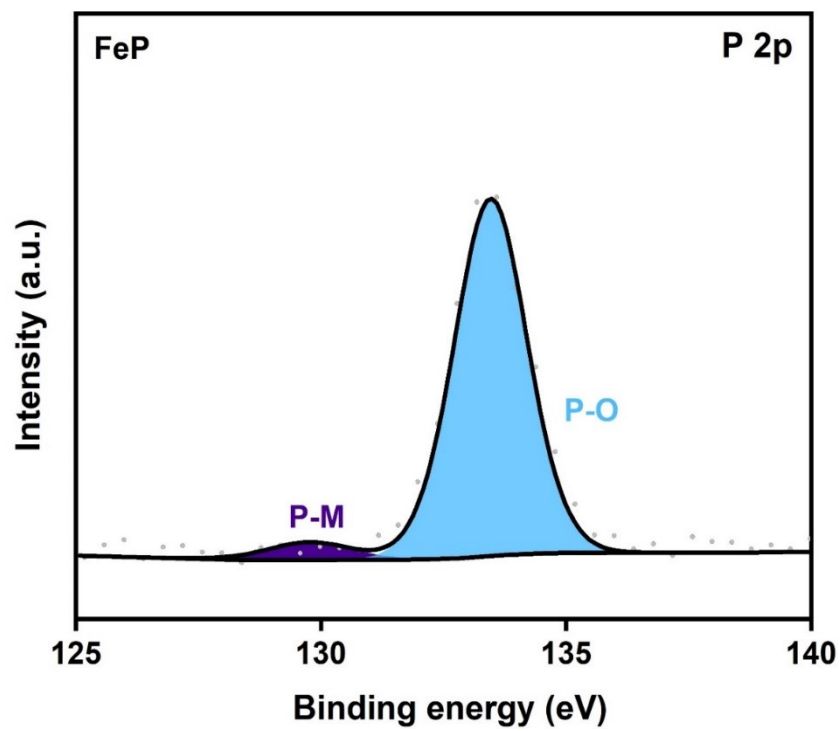


Figure S4. XPS P 2p spectrum of FeP.

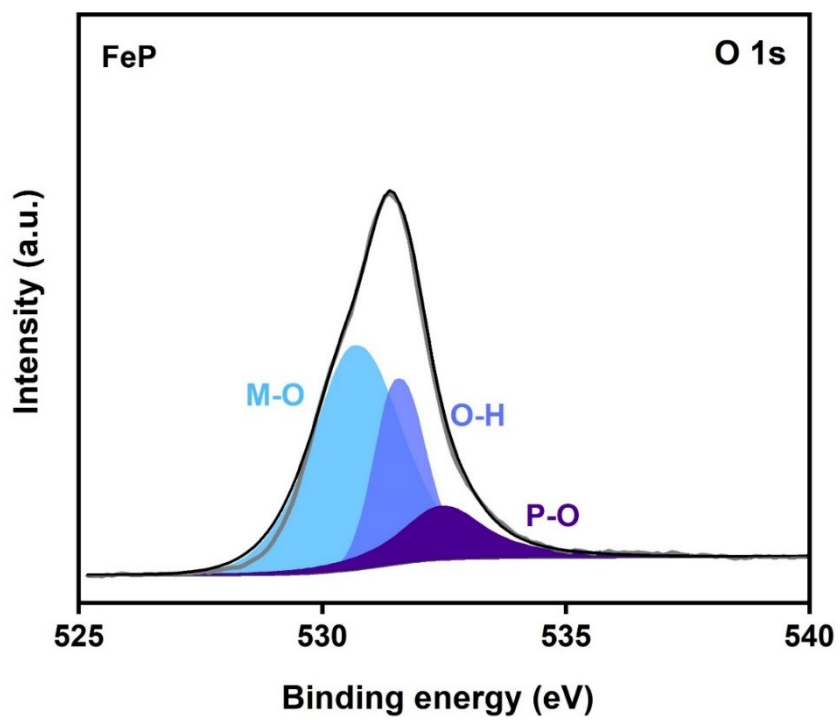


Figure S5. XPS O 1s spectrum of FeP.

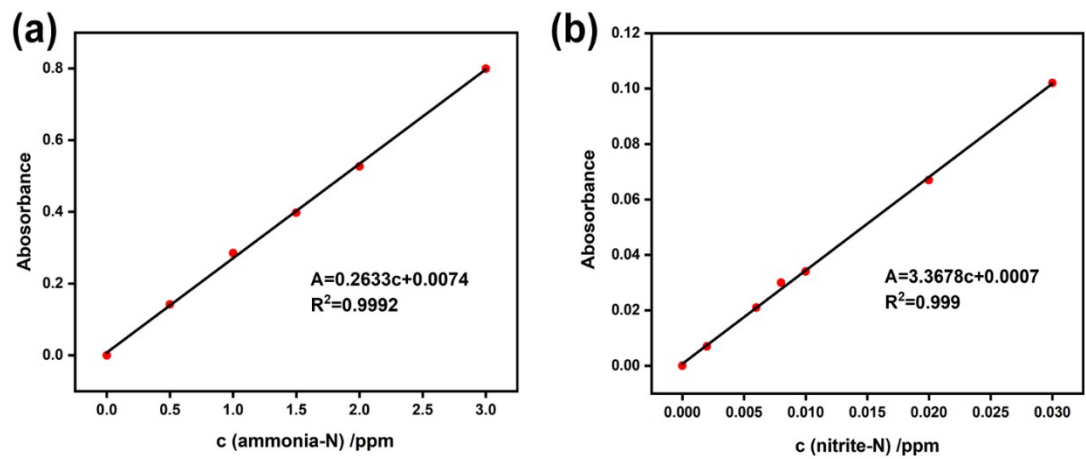


Figure S6. The concentration-absorbance calibration curves of (a) ammonia-N, (b) nitrite-N.

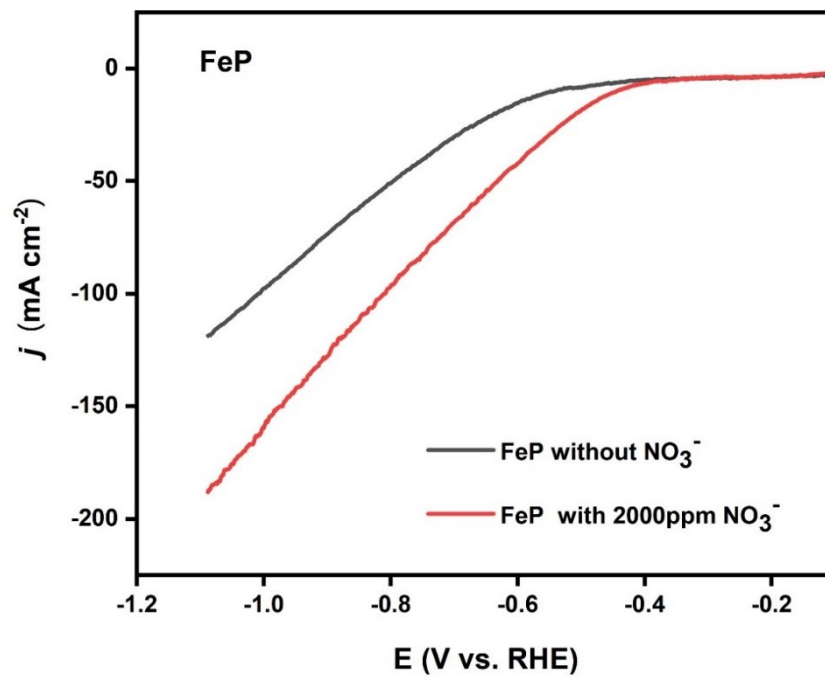


Figure S7. LSV curves of FeP tested in 0.25 M Na<sub>2</sub>SO<sub>4</sub> with or without 2000 ppm NO<sub>3</sub><sup>-</sup>.

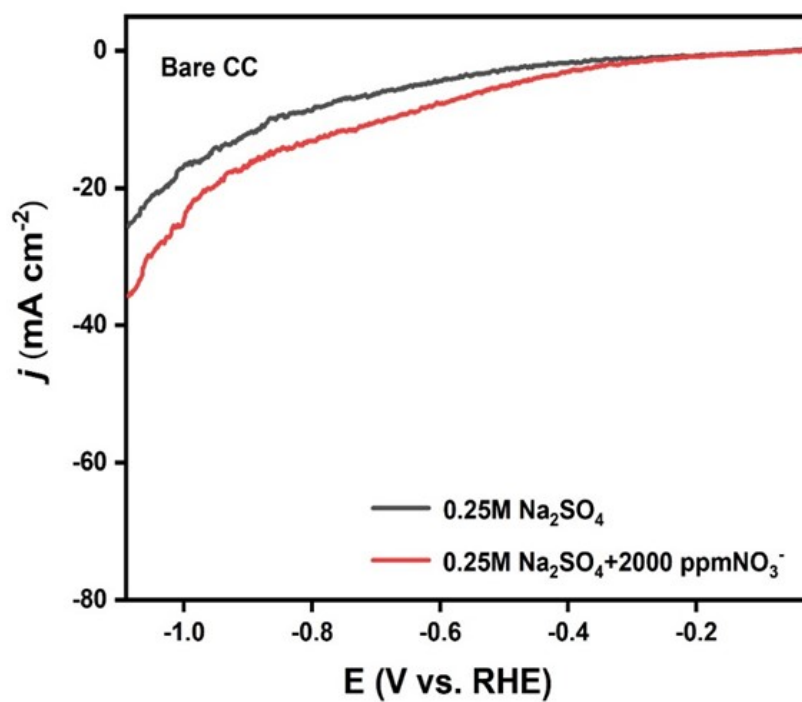


Figure S8. LSV curves of bare CC tested in 0.25 M Na<sub>2</sub>SO<sub>4</sub> with or without 2000 ppm NO<sub>3</sub><sup>-</sup>.

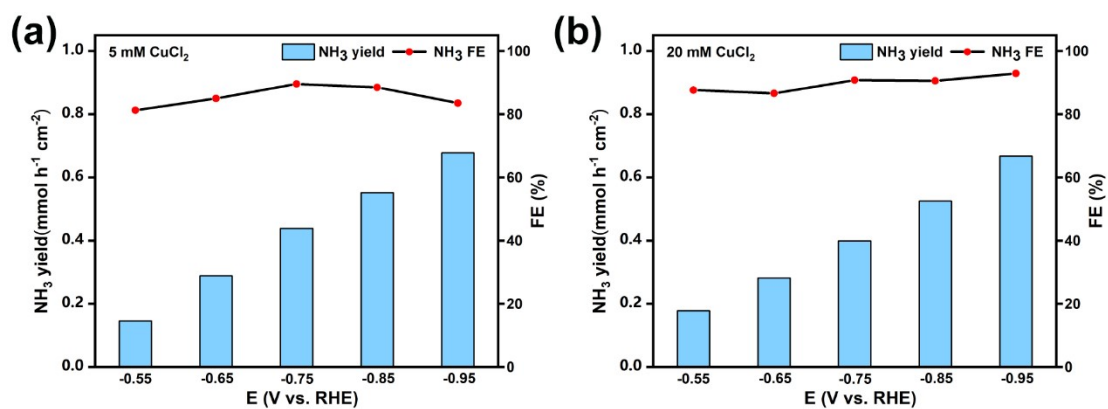


Figure S9.  $\text{NH}_3$  yields and FEs of Cu-FeP samples with different Cu contents prepared via using (a) 5 mM  $\text{CuCl}_2$ , and (b) 20 mM  $\text{CuCl}_2$  solution in the cation exchange step tested in 0.25 M  $\text{Na}_2\text{SO}_4$  with 2000 ppm  $\text{NO}_3^-$ .

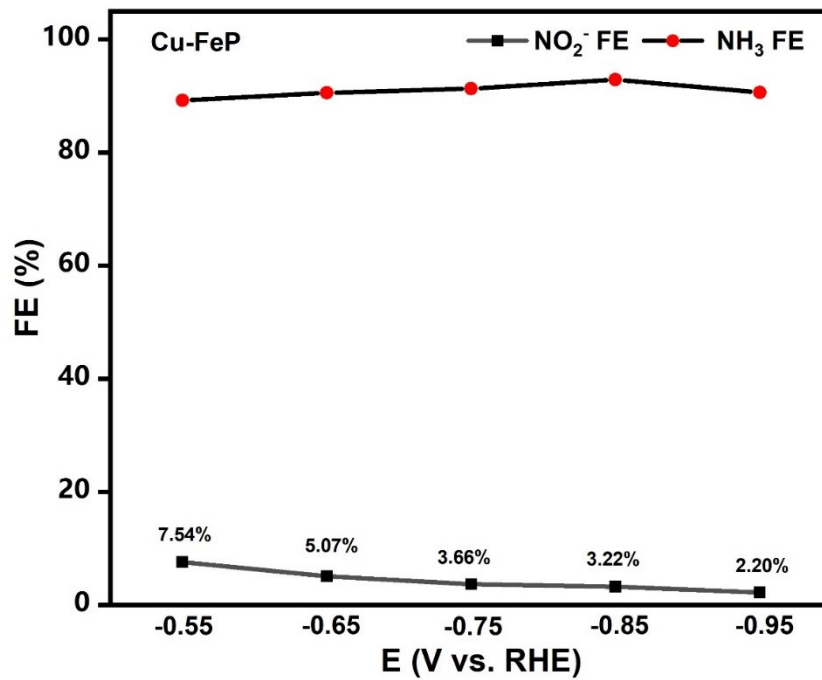


Figure S10. FEs of  $\text{NH}_3$ , and  $\text{NO}_2^-$  on Cu-FeP at different applied potentials.

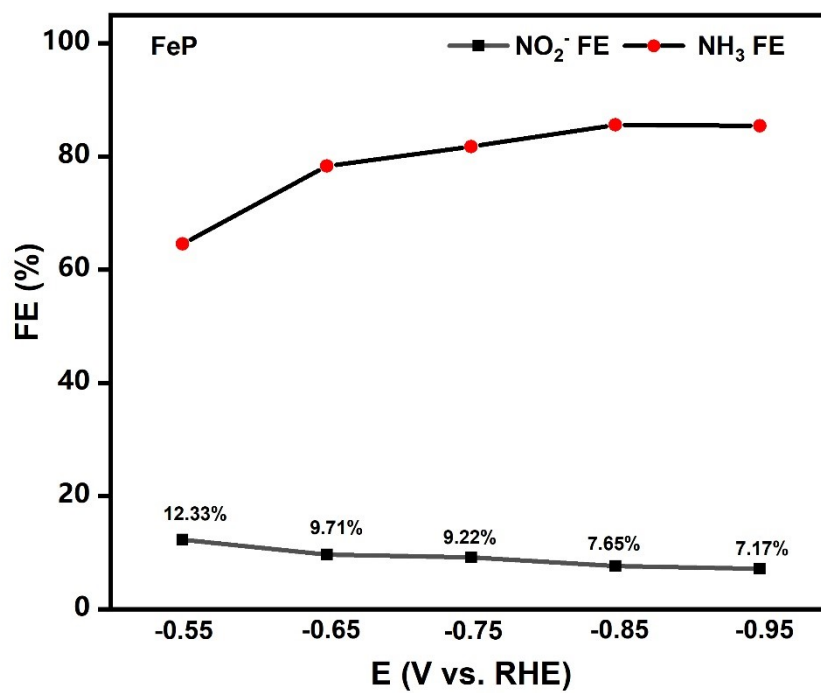


Figure S11. FEs of  $\text{NH}_3$ , and  $\text{NO}_2^-$  on FeP at different applied potentials.

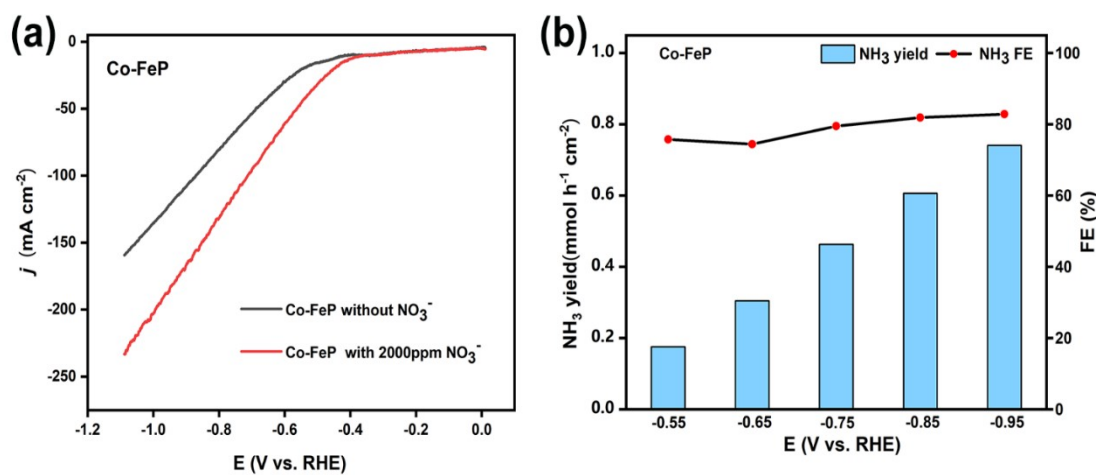


Figure S12. (a) LSV curves of Co-FeP tested in 0.25 M  $\text{Na}_2\text{SO}_4$  with or without 2000 ppm  $\text{NO}_3^-$ . (b)  $\text{NH}_3$  yields and FEs of Co-FeP sample tested at different applied potentials in 0.25 M  $\text{Na}_2\text{SO}_4$  with 2000 ppm  $\text{NO}_3^-$ .

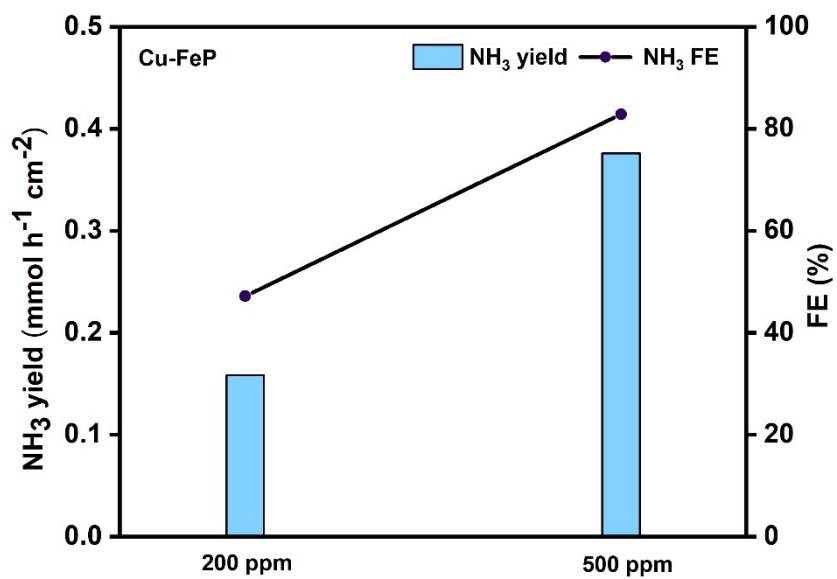


Figure S13. NH<sub>3</sub> yields and FEs of Cu-FeP tested at  $-0.85\text{V vs. RHE}$  in  $0.25\text{ M Na}_2\text{SO}_4$  with low  $\text{NO}_3^-$  concentrations.

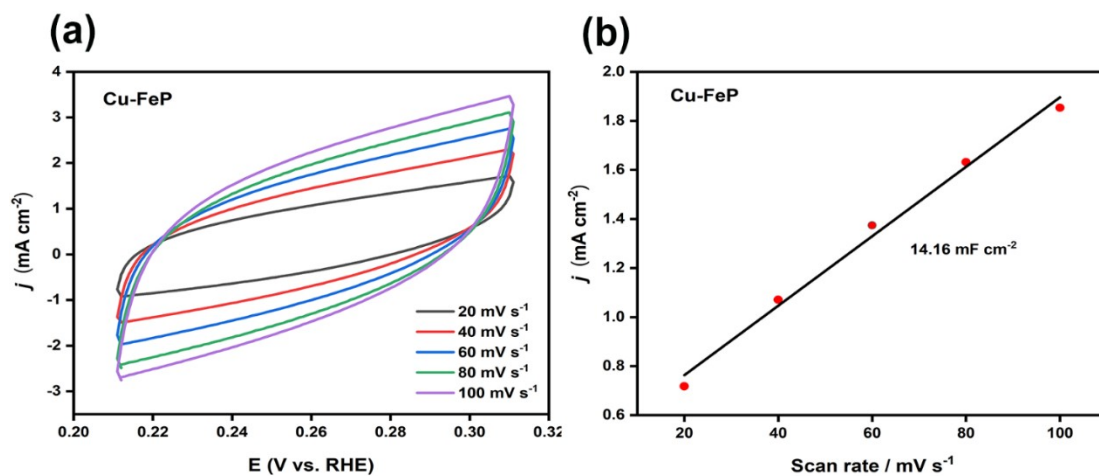


Figure S14. (a) Cyclic voltammograms (CV) curves for Cu-FeP at the scan rates from 20 to 100 mV s<sup>-1</sup>. (b) Current density as a function of the scan rate to give the double-layer capacitance ( $C_{dl}$ ) for Cu-FeP.

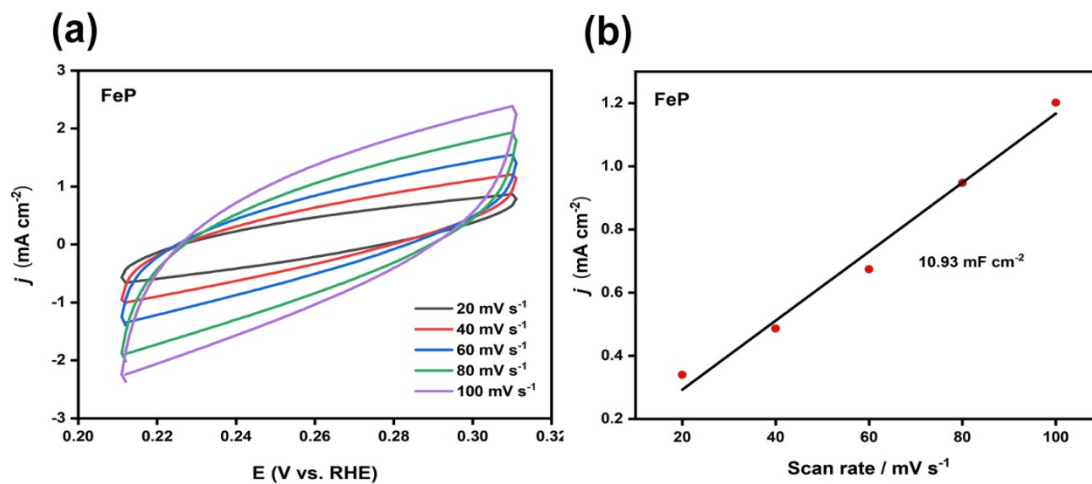


Figure S15. (a) Cyclic voltammograms (CV) curves for FeP at the scan rates from 20 to 100 mV s<sup>-1</sup>. (b) Current density as a function of the scan rate to give the double-layer capacitance ( $C_{dl}$ ) for FeP.

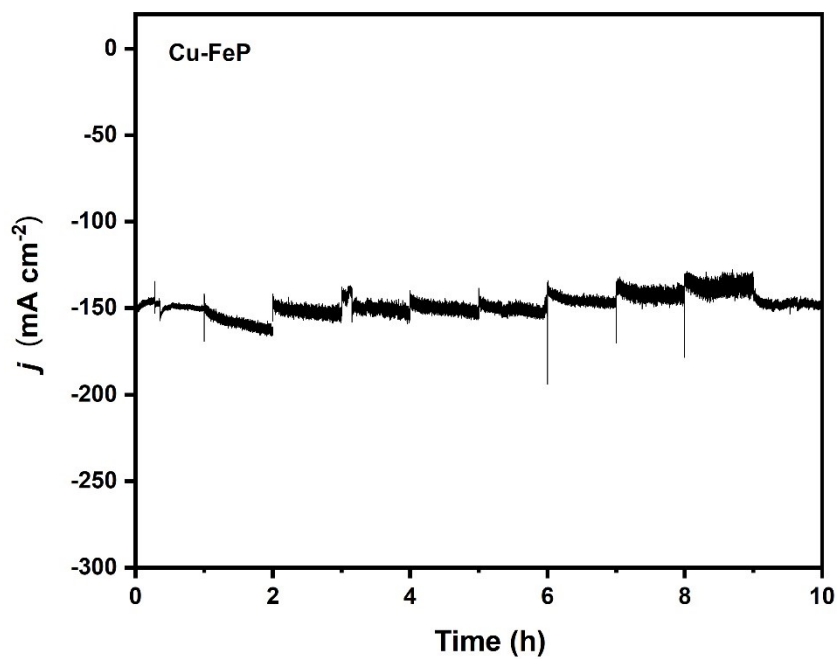


Figure S16. Chronoamperometry curves of Cu-FeP performed at  $-0.85$  V vs. RHE in  $0.25$  M  $\text{Na}_2\text{SO}_4$  with  $2000$  ppm  $\text{NO}_3^-$ .

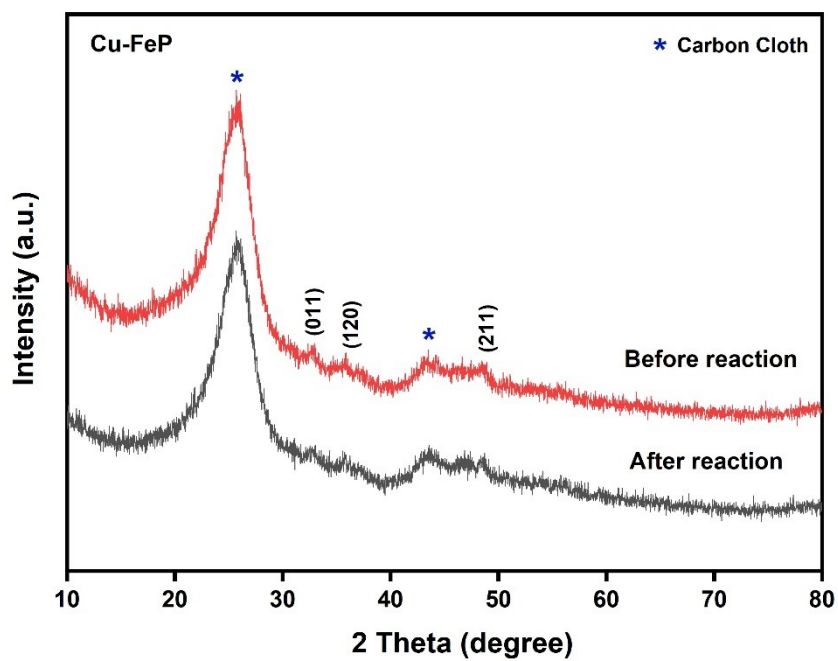


Figure S17. XRD patterns of Cu-FeP sample before and after the  $\text{NO}_3\text{RR}$  cycling test.

Table 1. Summary of the electrochemical performance of some reported nitrate reduction electrocatalysts in the neutral electrolytes.

Catalyst	Electrolyte	Potential	Performance	Ref.
Cu-FeP	0.25 M Na <sub>2</sub> SO <sub>4</sub> 2000 ppm NO <sub>3</sub> <sup>-</sup>	-0.95 V (vs. RHE)	FE = 92.5% NH <sub>3</sub> yield = 0.787 mmol h <sup>-1</sup> cm <sup>-2</sup>	This work
TiO <sub>2-x</sub>	0.50 M Na <sub>2</sub> SO <sub>4</sub> 0.50 mg L <sup>-1</sup> NO <sub>3</sub> <sup>-</sup>	-1.6 V (vs. SCE)	FE = 85% NH <sub>3</sub> yield = 0.045 mmol h <sup>-1</sup> mg <sup>-1</sup>	1
Fe SAC	0.10 M K <sub>2</sub> SO <sub>4</sub> 0.50 M NO <sub>3</sub> <sup>-</sup>	-0.66 V (vs. RHE)	FE = 75% NH <sub>3</sub> yield = 0.460 mmol h <sup>-1</sup> cm <sup>-2</sup>	2
Cu/Cu <sub>2</sub> O	0.50 M Na <sub>2</sub> SO <sub>4</sub> 200 ppm NO <sub>3</sub> <sup>-</sup>	-0.85 V (vs. RHE)	FE = 95.8% NH <sub>3</sub> yield = 0.245 mmol h <sup>-1</sup> cm <sup>-2</sup>	3
Co/CoO NSA	0.10 M K <sub>2</sub> SO <sub>4</sub> 200 ppm NO <sub>3</sub> <sup>-</sup>	-1.3 V (vs. SCE)	FE = 93.8% NH <sub>3</sub> yield = 0.200 mmol h <sup>-1</sup> cm <sup>-2</sup>	4
Cu-Co <sub>3</sub> O <sub>4-x</sub>	0.25 M Na <sub>2</sub> SO <sub>4</sub> 2000 ppm NO <sub>3</sub> <sup>-</sup>	-1.05 V (vs. RHE)	FE = 88.93% NH <sub>3</sub> yield = 0.830 mmol h <sup>-1</sup> cm <sup>-2</sup>	5
meso-PdN NCs	0.10 M Na <sub>2</sub> SO <sub>4</sub> 0.005 M NO <sub>3</sub> <sup>-</sup>	-0.7 V (vs. RHE)	FE = 96.1% NH <sub>3</sub> yield = 0.220 mmol h <sup>-1</sup> cm <sup>-2</sup>	6
Fe-SnS <sub>2</sub>	0.50 M Na <sub>2</sub> SO <sub>4</sub> 0.10 M NO <sub>3</sub> <sup>-</sup>	-0.7 V (vs. RHE)	FE = 85.6% NH <sub>3</sub> yield = 0.434 mmol h <sup>-1</sup> cm <sup>-2</sup>	7
Defect-rich Cu	0.50 M K <sub>2</sub> SO <sub>4</sub> 50 ppm NO <sub>3</sub> <sup>-</sup>	-1.3 V (vs. SCE)	FE = 85.5% NH <sub>3</sub> yield = 0.046 mmol h <sup>-1</sup> mg <sup>-1</sup>	8
CuCl/TiO <sub>2</sub>	0.5 M Na <sub>2</sub> SO <sub>4</sub> 100 ppm NO <sub>3</sub> <sup>-</sup>	-1.0 V (vs. RHE)	FE = 88% NH <sub>3</sub> yield = 0.107 mmol h <sup>-1</sup> cm <sup>-2</sup>	9
Pd	0.10 M Na <sub>2</sub> SO <sub>4</sub> 0.10 M NO <sub>3</sub> <sup>-</sup>	-0.7 V (vs. RHE)	FE = 79.91% NH <sub>3</sub> yield = 0.549 mmol h <sup>-1</sup> cm <sup>-2</sup>	10

## References

1. R. Jia, Y. Wang, C. Wang, Y. Ling, Y. Yu and B. Zhang, *ACS Catal.*, 2020, **10**, 3533–3540.
2. Z.-Y. Wu, M. Karamad, X. Yong, Q. Huang, D. A. Cullen, P. Zhu, C. Xia, Q. Xiao, M. Shakouri, F.-Y. Chen, J. Y. Kim, Y. Xia, K. Heck, Y. Hu, M. S. Wong, Q. Li, I. Gates, S. Siahrostami and H. Wang, *Nat. Commun.*, 2021, **12**, 2870.
3. Y. Wang, W. Zhou, R. Jia, Y. Yu and B. Zhang, *Angew. Chem. Int. Ed.*, 2020, **59**, 5350–5354.
4. Y. Yu, C. Wang, Y. Yu, Y. Wang and B. Zhang, *Sci. China Chem.*, 2020, **63**, 1469–1476.
5. B. Li, P. Xue, Y. Bai, Q. Tang, M. Qiao and D. Zhu, *Chem. Commun.*, 2023, **59**, 5086–5089.
6. L. Sun and B. Liu, *Adv. Mater.*, 2023, **35**, 2207305.
7. K. Chen, Y. Luo, P. Shen, X. Liu, X. Li, X. Li and K. Chu, *Dalton Trans.*, 2022, **51**, 10343–10350.
8. Y. Xu, M. Wang, K. Ren, T. Ren, M. Liu, Z. Wang, X. Li, L. Wang and H. Wang, *J. Mater. Chem. A*, 2021, **9**, 16411–16417.
9. W.-J. Sun, H.-Q. Ji, L.-X. Li, H.-Y. Zhang, Z.-K. Wang, J.-H. He and J.-M. Lu, *Angew. Chem. Int. Ed.*, 2021, **60**, 22933–22939.
10. Y. Han, X. Zhang, W. Cai, H. Zhao, Y. Zhang, Y. Sun, Z. Hu, S. Li, J. Lai and L. Wang, *J. Colloid Interface Sci.*, 2021, **600**, 620–628.